

LETTERS

STIM1 is a Ca^{2+} sensor that activates CRAC channels and migrates from the Ca^{2+} store to the plasma membrane

Shenyuan L. Zhang¹, Ying Yu¹, Jack Roos², J. Ashot Kozak¹, Thomas J. Deerinck³, Mark H. Ellisman³, Kenneth A. Stauderman² & Michael D. Cahalan¹

As the sole Ca^{2+} entry mechanism in a variety of non-excitable cells, store-operated calcium (SOC) influx is important in Ca^{2+} signalling and many other cellular processes^{1–3}. A calcium-release-activated calcium (CRAC) channel in T lymphocytes is the best-characterized SOC influx channel^{4–6} and is essential to the immune response, sustained activity of CRAC channels being required for gene expression and proliferation^{7–10}. The molecular identity and the gating mechanism of SOC and CRAC channels have remained elusive. Previously we identified *Stim* and the mammalian homologue STIM1 as essential components of CRAC channel activation in *Drosophila* S2 cells and human T lymphocytes¹¹. Here we show that the expression of EF-hand mutants of *Stim* or STIM1 activates CRAC channels constitutively without changing Ca^{2+} store content. By immunofluorescence, EM localization and surface biotinylation we show that STIM1 migrates from endoplasmic-reticulum-like sites to the plasma membrane upon depletion of the Ca^{2+} store. We propose that STIM1 functions as the missing link between Ca^{2+} store depletion and SOC influx, serving as a Ca^{2+} sensor that translocates upon store depletion to the plasma membrane to activate CRAC channels.

We previously characterized a SOC current in *Drosophila* S2 cells with biophysical properties similar to CRAC channels in human T cells¹². More recently, *Stim* was identified in an RNA-mediated interference (RNAi)-based screen with the SERCA (sarcolemmal/endoplasmic reticulum Ca^{2+} ATPase) pump inhibitor thapsigargin (TG) to evoke SOC influx in *Drosophila* S2 cells¹¹. Uniquely among the 170 candidate genes that were screened, including all *trp*-related genes, RNAi-mediated suppression of *Stim* inhibited the Ca^{2+} influx evoked by TG. By single-cell imaging of cytosolic Ca^{2+} concentration ($[\text{Ca}^{2+}]_i$) and patch clamp analysis, we confirmed a functional requirement for *Stim*, and for the human homologue STIM1, to mediate CRAC channel activity in S2 cells and in Jurkat T cells, respectively. *Drosophila Stim* and mammalian STIM1 (collectively referred to here as Stim1) are modular type I transmembrane proteins with an EF-hand motif near the amino terminus located in the lumen of the endoplasmic reticulum (ER) or outside the cell (Supplementary Fig. 1)¹³. Because Stim1 does not resemble any known ion channel, the presence of the EF-hand motif and its localization indicated that Stim1 might function as a sensor of the ER Ca^{2+} store. According to this proposal, Ca^{2+} binding to the EF-hand domain of Stim1 within the lumen of the Ca^{2+} store would keep CRAC channels in the plasma membrane closed.

To test this possibility, full-length STIM1 and *Stim* cDNA were cloned from RBL cells and S2 cells and placed into appropriate

expression vectors. Mutants in the EF-hand region were prepared, two for STIM1 and four for *Stim*, on residues known to be critical for Ca^{2+} binding^{14,15}. Overexpression of wild-type (WT) or mutant Stim1 after transient transfection was confirmed by western blotting (Supplementary Fig. 2). In single-cell Ca^{2+} imaging experiments, overexpression of WT Stim1 produced no significant difference in resting $[\text{Ca}^{2+}]_i$, TG-independent Ca^{2+} influx or TG-evoked store release compared with control blank-transfected cells (Jurkat cells are shown in Fig. 1, S2 cells in Supplementary Fig. 3). A modest increase in TG-dependent (store-operated) Ca^{2+} influx was seen in Jurkat T cells (Fig. 1b) but not in S2 cells, consistent with the hypothesis that Stim1 by itself is not a functional CRAC channel. In contrast, Jurkat or S2 cells transfected with the EF-hand mutants bore two severe phenotypes: resting $[\text{Ca}^{2+}]_i$ and TG-independent Ca^{2+} influx were increased from about 50 nM to more than 200 nM on average. Histograms of resting $[\text{Ca}^{2+}]_i$ show that expression of EF-hand mutants increased resting $[\text{Ca}^{2+}]_i$ to more than 600 nM in many individual cells (Supplementary Fig. 4). The Ca^{2+} release transient, obtained by adding TG in zero- Ca^{2+} solution, was not changed (Supplementary Fig. 5), showing that the Ca^{2+} store content was not affected. To test whether the high values of resting $[\text{Ca}^{2+}]_i$ and enhanced TG-independent Ca^{2+} influx were caused by constitutively opened CRAC channels, 2-aminoethyl diphenyl borate, SKF96365 and Gd^{3+} were applied as pharmacological tools that block CRAC channels in Jurkat cells and in S2 cells^{2,3,12,16–18}. Each of these agents inhibited TG-evoked SOC influx in control cells and, at the same concentrations, all three inhibited both the high resting Ca^{2+} concentration and the enhanced TG-independent Ca^{2+} influx in Jurkat and S2 cells transfected with EF-hand mutants (Fig. 1g–i, and Supplementary Fig. 3c). These results demonstrate that CRAC channels in Jurkat or S2 cells are constitutively opened by overexpression of Stim1 EF-hand mutants.

In addition to affecting resting $[\text{Ca}^{2+}]_i$, expression of *Stim* EF-hand mutants arrested the growth of S2 cells, whereas overexpressing WT *Stim* had a small effect compared with that in S2 cells undergoing blank transfection (Supplementary Fig. 6). Most S2 cells overexpressing *Stim* EF-hand mutants were stained by annexin V, an early marker for the exposure of phosphatidylserine that occurs during apoptosis¹⁹. The growth arrest and apoptosis were probably triggered by abnormally high resting $[\text{Ca}^{2+}]_i$ (refs 19–21). A similar but milder growth defect in Jurkat cells overexpressing STIM1 EF-hand mutants was also observed.

How does STIM1 regulate the activity of CRAC channels? The subcellular localization of STIM1 was examined by

¹Department of Physiology and Biophysics and Center for Immunology, University of California, Irvine, California 92697, USA. ²TorreyPines Therapeutics, Inc., La Jolla, California 92037, USA. ³National Center for Microscopy and Imaging Research, Center for Research in Biological Structure and the Department of Neurosciences, University of California, San Diego, La Jolla, California 92093, USA.

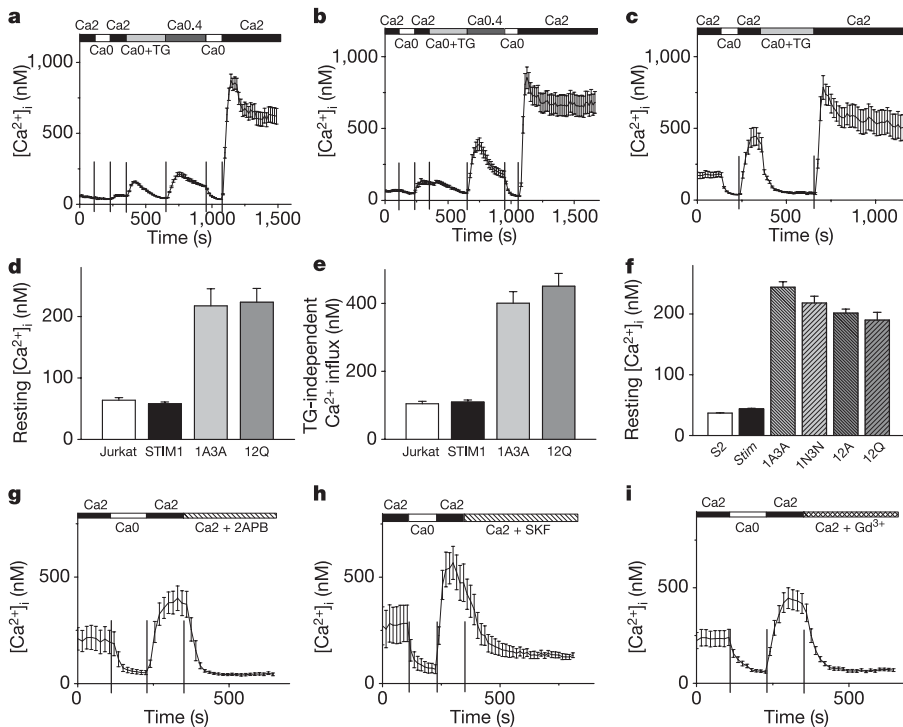


Figure 1 | Constitutive activation of CRAC channels by expression of EF-hand mutants of Stim or STIM1. **a–c**, Average $[Ca^{2+}]_i$ responses in blank-transfected Jurkat cells (**a**; $n = 59$), Jurkat cells overexpressing WT STIM1 (**b**; $n = 29$) and Jurkat cells overexpressing STIM1 EF12Q (**c**; $n = 18$). Cells were bathed in solutions as indicated: the number after ‘Ca’ reflects the Ca^{2+} concentration in mM. **d–f**, Resting $[Ca^{2+}]_i$ in Jurkat cells (**d**; from left to right: $n = 114$, $n = 171$, $n = 61$ and $n = 65$); TG-independent Ca^{2+} influx in Jurkat cells (**e**; $n = 114$, $n = 136$, $n = 61$ and $n = 42$); and resting $[Ca^{2+}]_i$ in S2 cells (**f**; $n = 392$, $n = 568$, $n = 425$, $n = 149$, $n = 316$ and $n = 102$). **g–i**, Effects of CRAC channel blockers 2-aminoethylidiphenyl borate (2APB) (**g**, $50 \mu M$), SKF96365 (**h**, $20 \mu M$) and Gd^{3+} (**i**, $1 \mu M$) on TG-independent Ca^{2+} influx in Jurkat cells. The EF-hand mutants used were 12Q (**g**, $n = 16$), 12Q (**h**, $n = 8$) and 1A3A (**i**, $n = 28$). Error bars indicate s.e.m.

immunofluorescence staining of Jurkat cells overexpressing either WT STIM1 or STIM1 EF-hand mutants. In cells that overexpressed STIM1, most of the staining appeared within the ring of cytoplasm surrounding the nucleus, and very little was on the cell surface (Fig. 2a), which is consistent with a previous surface biotinylation study²². In contrast, EF-hand mutant STIM1 proteins that induce constitutive activation of CRAC channels were located predominantly on the surface membrane (Fig. 2b). Comparison with co-transfected green fluorescent protein (GFP) helped to define STIM1 or EF-hand mutant STIM1 at or below the cell surface. We reasoned that the altered localization of EF-hand mutants to the plasma membrane could result from their inability to bind Ca^{2+} within the intracellular store. Translocation of WT Stim1 from the Ca^{2+} store to the plasma membrane might therefore be a key event in the signalling pathway that activates CRAC channels. This hypothesis was supported by immunofluorescence staining of endogenous STIM1 in Jurkat T cells (Fig. 2c) and also in RBL cells, resting T cells from human donors and PC12 cells (Supplementary Figs 7 and 8). In cells pretreated with $1 \mu M$ TG in zero- Ca^{2+} external solution to deplete the Ca^{2+} store without causing a large increase in cytosolic $[Ca^{2+}]_i$, ‘hotspots’ of STIM1 staining were found at the cell surface, whereas a predominantly cytosolic distribution of STIM1 staining was seen in control cells bathed in Ringer solution containing $2 mM Ca^{2+}$. In the control condition with Ca^{2+} stores full, STIM1 co-localized with ER markers (SERCA2 and protein disulphide isomerase) in Jurkat and in RBL cells, respectively, but after store depletion STIM1 accumulated in hotspots at the surface, and co-localization in the ER was less extensive (Fig. 2c, and Supplementary Fig. 8). STIM1 translocation kinetics were evaluated by fixing cells at different time points after treatment with TG or cyclopiazonic acid (CPA), another SERCA pump inhibitor that depletes ER Ca^{2+} stores and triggers SOC influx²³ (Fig. 2d and Supplementary Fig. 9a). When Ca^{2+} -store depletion was initiated, STIM1 moved rapidly to the surface membrane, reaching near-maximal surface expression within about 5 min and remaining on the surface for at least 40 min. For comparison, the inhibition of SERCA pumps activated CRAC currents with a somewhat more rapid time course in perforated patch recordings. Current begins to develop when STIM1 translocation is first observed, and

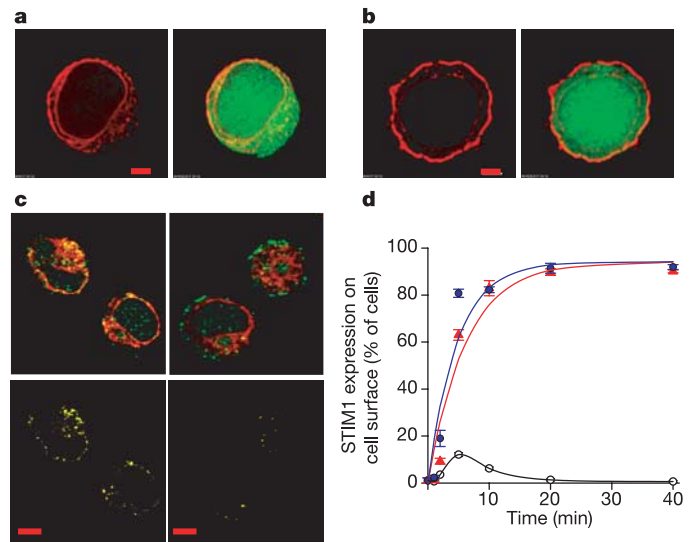


Figure 2 | Mutations in EF-hand motif or store depletion induce STIM1 translocation to the plasma membrane. **a, b**, STIM1 (red) immunofluorescence staining of Jurkat cells transfected with WT STIM1 (**a**) or EF1A3A STIM1 (**b**), in Ringer solution containing $2 mM Ca^{2+}$ (left). EGFP (green) was co-transfected to define the cytoplasmic region (right). Scale bar, $2 \mu m$. **c**, STIM1 (green) and SERCA2 (red) immunofluorescence staining of Jurkat cells in $2 mM Ca^{2+}$ Ringer solution (left) or $1 \mu M$ TG in zero- Ca^{2+} solution for 10 min (right). Note the separation of STIM1 at the cell surface (top right). Bottom: co-localization images (yellow) depicting pixels that contained both STIM1 and ER fluorescence. Note reduced co-localization caused by STIM1 translocation in TG-treated cells. Scale bar, $5 \mu m$. **d**, Time course of STIM1 translocation triggered by $1 \mu M$ TG (filled circles) or $10 \mu M$ CPA (triangles), represented by the percentage of cells with strong surface fluorescence. Open circles, $2 mM Ca^{2+}$. An average of 315 cells were counted for each time point. Time constants: 4.7 min (TG), 6.1 min (CPA). Error bars indicate s.e.m.

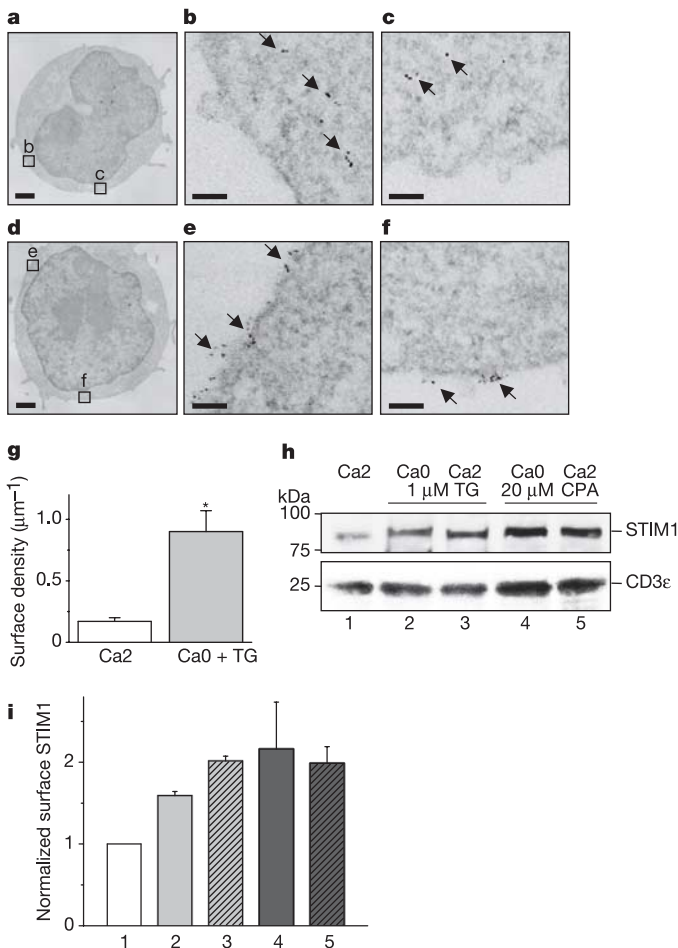


Figure 3 | Subcellular distribution of STIM1 before and after store depletion: immunoelectron microscopy and surface biotinylation. **a**, Quantum-dot-labelled STIM1 in control Jurkat cells bathed in Ringer solution containing 2 mM Ca²⁺. **b, c**, Enlargements of the boxed areas in **a**. **d**, STIM1 in Jurkat cells pretreated for 15 min with 1 μM TG in zero-Ca²⁺ solution. **e, f**, Enlarged regions of **d** showing clustered STIM1 distribution on the plasma membrane. Scale bar, 1 μm (**a, d**); 0.1 μm (**b, c, e, f**). **g**, STIM1 surface density, pooled data from control cells ($n = 14$) and store-depleted cells ($n = 13$); asterisk denotes $P < 0.01$ compared with controls. Ca₂, 2 mM Ca²⁺; Ca₀, zero Ca²⁺. **h**, Jurkat cells were treated for 30 min as indicated. Biotinylated proteins were detected by antibodies against STIM1 (top) and CD3 ϵ (bottom). **i**, Quantification of biotinylation experiments: there was a 1.6–2.2-fold increase upon store depletion. Error bars indicate s.e.m.

reaches a peak at 160 ± 66 s (mean \pm s.d., $n = 6$ cells; Supplementary Fig. 8b), when STIM1 translocation rate is maximal. Additional experiments, summarized in Supplementary Fig. 9b–d, indicated that STIM1 surface translocation also occurred when [Ca²⁺]_i was elevated accompanying store depletion by treatment with TG in 2 mM Ca²⁺ external solution, but did not occur in cells treated with zero-Ca²⁺ solution in the absence of TG or in cells treated with 2 mM Ca²⁺ plus dimethylsulphoxide used to dissolve TG. Thus, depletion of intracellular Ca²⁺ stores is sufficient to trigger translocation of STIM1 proteins to the plasma membrane, indicating a possible mechanistic link to CRAC channel activation.

The translocation of STIM1 was further confirmed by immunoelectron microscopy, using quantum-dot-conjugated second antibodies after polyclonal anti-STIM1 antibodies to reveal STIM1 protein with single-molecule resolution. In control cells bathed in Ringer solution containing 2 mM Ca²⁺, most quantum dots were located in the lumen of smooth ER-like vesicular structures within the cytosol and occasionally at the cell surface (Fig. 3a–c). In contrast,

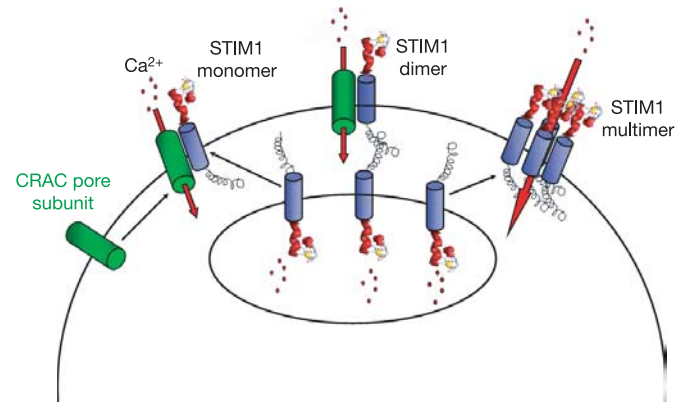


Figure 4 | Models of STIM1 function. Upon store depletion, STIM1 located in the ER unbinds Ca²⁺ and translocates to the plasma membrane to activate CRAC channel subunits that are already in the plasma membrane (left), form junctions between the Ca²⁺ store and the plasma membrane (middle) or assemble to form functional CRAC channels (right).

in TG-treated cells quantum dots appeared in clusters on the plasma membrane (Fig. 3d–f). The STIM1 surface density, with or without Ca²⁺-store depletion, was determined by counting the number of quantum dots normalized to the linear distance along the plasma membrane. A fivefold increase in STIM1 surface density was obtained after treatment with TG to induce store depletion (Fig. 3g). Moreover, an increase in surface-accessible STIM1 was also detected by biotinylation (Fig. 3h, i).

The results can be summarized in two main conclusions: first, CRAC channels are activated when Stim1 is unable to bind Ca²⁺ within the store, either after Ca²⁺ release or if the EF-hand mutant is expressed; and second, Stim1 translocates to the plasma membrane upon Ca²⁺ store depletion. Previously we showed that STIM1 also regulates SOC influx in HEK-293 and SH-SY5Y cells¹¹. In addition, while this paper was in review, a report from Liou *et al.* showed that STIM1 has a function in the regulation of SOC influx in HeLa cells²⁴. This group also reported redistribution (but not membrane insertion) of YFP-tagged STIM1 upon store depletion, but did not examine endogenous STIM1. By showing translocation and membrane insertion of endogenous STIM1, our data suggest a crucial link to the functional role of STIM1. On the basis of these findings we propose a calcium sensor model to account for the role of Stim1 in regulating SOC influx. The proposed model is a modification of a vesicle fusion hypothesis for CRAC channel activation, in which Stim1 is the element that translocates. As illustrated in Fig. 4, Stim1 is initially located in the membrane of the Ca²⁺ store, with its low-affinity EF hand inside the lumen sensing Ca²⁺ and stabilized by bound Ca²⁺ when the store is full. When the store is depleted by inositol-1,4,5-trisphosphate-induced Ca²⁺ release or by inhibition of the SERCA pump, Ca²⁺ dissociates and Stim1 moves to the plasma membrane, presumably in vesicles that may insert into the membrane. Mutation of the EF hand mimics Ca²⁺ store depletion, initiating the translocation and activation of CRAC channels. Once Stim1 is at the cell surface it can activate the CRAC channel in one of three ways: it can interact with a putative pore-forming subunit, it can activate Ca²⁺ influx by means of conformational coupling through its coiled-coil domain, or it can assemble with additional Stim1 monomers and perhaps other components to form a unique functional Ca²⁺ channel. In addition to mechanistic insights, Stim1 may provide a biochemical handle with which to identify additional components of the translocation mechanism and the CRAC channel pore.

METHODS

Cell culture and transfection. *Drosophila* S2 cells (Invitrogen) were propagated at 27 °C in Schneider's medium (Invitrogen) supplemented with 12.5% FCS and 1% glutamine. Cells were seeded at a density of 10^6 cells ml⁻¹ and passed when

the cells achieved a density of about 6×10^6 cells ml^{-1} . Jurkat T cells (ATCC) were maintained and propagated as detailed by the ATCC. RBL-2H3 cells and PC12 cells were cultured in Eagle's MEM and DMEM, respectively, supplemented with 10% fetal bovine serum in 5% CO_2 -humidified atmosphere at 37 °C. Cells were passed twice weekly. Human peripheral T lymphocytes were isolated from the blood of healthy volunteers with the use of CD3⁺ RosetteSep (StemCell Technologies) and Histopaque 1077 (Sigma) and cultured in RPMI supplemented with 10% fetal bovine serum. S2 cells and Jurkat cells were transfected (see clones described in Supplementary Information) using a Nucleofector (Amaxa) in accordance with the manufacturer's protocol. Forty-eight hours after transfection, protein expression was confirmed by western blotting, and cells were used for $[\text{Ca}^{2+}]_i$ imaging, immunocytochemistry and apoptosis assays.

Antibodies and western blotting. Cell extracts were prepared by washing the cells with PBS and then extracting proteins with lysis buffer (in mM): 10 Tris, 3 CaCl_2 , 2 MgCl_2 , 2.5% Nonidet P40, pH 7.5. Protein concentration was determined with the Pierce BCA Protein Reagent Kit. The extract was prepared for SDS-PAGE analysis by the addition of 4 × sample buffer (Invitrogen). Samples were resolved by SDS-PAGE and analysed by standard western blotting techniques. STIM1 polyclonal antibodies against a carboxy-terminal peptide (STIM1-CT, DNGSIGETDSSPGRKKFPLKIFKPLKK) were used at a dilution of 1:2500. Monoclonal antibodies against glyceraldehyde3phosphate dehydrogenase were from Research Diagnostics and used at a dilution of 1:5000. Anti-V5/horseradish peroxidase monoclonal antibodies were from Invitrogen and used at a dilution of 1:5000. Proteins were detected by developing with the SuperSignal (Pierce) detection system.

Single-cell $[\text{Ca}^{2+}]_i$ imaging. Ratiometric $[\text{Ca}^{2+}]_i$ imaging experiments were performed on S2 and Jurkat cells with Fura-2 as described¹¹, using solution recipes indicated in Supplementary Table 1. Transfected cells were recognized by co-expressed enhanced green fluorescent protein (EGFP), using filters to avoid contamination of Fura-2 fluorescence by bleed-through of GFP fluorescence²⁵. Data were analysed with Metafluor software (Universal Imaging) and OriginPro 7.5 software (OriginLab) and are expressed as means ± s.e.m.

Immunocytochemistry, light and electron microscopy. Stained cells were viewed under a confocal laser scanning microscope LSM510 META (Zeiss) or DeltaVision RT Restoration Imaging System. Q-dot-labelled cells were fixed for 10 min in 2% glutaraldehyde and postfixed for 20 min in 1% osmium tetroxide. Cells were then washed in distilled water, then dehydrated in ethanol and embedded in Durcupan ACM epoxy resin and subsequently prepared and viewed by electron microscopy (Jeol 2000FX).

Surface biotinylation. Cell-surface STIM1 protein was detected by cell-surface biotinylation and purification, in accordance with the manufacturer's instructions (Pierce), by using a modified protocol²² as described in Supplementary Information. Data were quantified with ImageJ software (NIH) and normalized as means ± s.e.m.

Perforated patch recording. CRAC current was activated by CPA or TG in RBL cells during perforated-patch recording with amphotericin B (0.2 mg ml^{-1}) in the pipette. See Supplementary Information for pipette and external solutions and recording protocols.

Received 22 April; accepted 22 August 2005.

- Putney, J. W. Jr, Broad, L. M., Braun, F. J., Lievreumont, J. P. & Bird, G. S. Mechanisms of capacitative calcium entry. *J. Cell Sci.* **114**, 2223–2229 (2001).
- Putney, J. W. Jr Store-operated calcium channels: how do we measure them, and why do we care? [online]. *Sci. STKE* **2004** (243), pe37 (2004) (doi:10.1126/stke.2432004pe37).
- Lewis, R. S. Store-operated calcium channels. *Adv. Second Messenger Phosphoprotein Res.* **33**, 279–307 (1999).
- Parekh, A. B. & Putney, J. W. Jr Store-operated calcium channels. *Physiol. Rev.* **85**, 757–810 (2005).
- Lewis, R. S. & Cahalan, M. D. Mitogen-induced oscillations of cytosolic Ca^{2+} and transmembrane Ca^{2+} current in human leukemic T cells. *Cell Regul.* **1**, 99–112 (1989).
- Parekh, A. B. & Penner, R. Store depletion and calcium influx. *Physiol. Rev.* **77**, 901–930 (1997).

- Lewis, R. S. Calcium signalling mechanisms in T lymphocytes. *Annu. Rev. Immunol.* **19**, 497–521 (2001).
- Winslow, M. M., Neilson, J. R. & Crabtree, G. R. Calcium signalling in lymphocytes. *Curr. Opin. Immunol.* **15**, 299–307 (2003).
- Feske, S., Giltman, J., Dolmetsch, R., Staudt, L. M. & Rao, A. Gene regulation mediated by calcium signals in T lymphocytes. *Nature Immunol.* **2**, 316–324 (2001).
- Partiseti, M. *et al.* The calcium current activated by T cell receptor and store depletion in human lymphocytes is absent in a primary immunodeficiency. *J. Biol. Chem.* **269**, 32327–32335 (1994).
- Roos, J. *et al.* STIM1, an essential and conserved component of store-operated Ca^{2+} channel function. *J. Cell Biol.* **169**, 435–445 (2005).
- Yeromin, A. V., Roos, J., Stauderman, K. A. & Cahalan, M. D. A store-operated calcium channel in *Drosophila* S2 cells. *J. Gen. Physiol.* **123**, 167–182 (2004).
- Williams, R. T. *et al.* Identification and characterization of the STIM (stromal interaction molecule) gene family: coding for a novel class of transmembrane proteins. *Biochem. J.* **357**, 673–685 (2001).
- Beckingham, K. Use of site-directed mutations in the individual Ca^{2+} -binding sites of calmodulin to examine Ca^{2+} -induced conformational changes. *J. Biol. Chem.* **266**, 6027–6030 (1991).
- Nakayama, S. & Kretsinger, R. H. Evolution of the EF-hand family of proteins. *Annu. Rev. Biophys. Biomol. Struct.* **23**, 473–507 (1994).
- Ross, P. E. & Cahalan, M. D. Ca^{2+} influx pathways mediated by swelling or stores depletion in mouse thymocytes. *J. Gen. Physiol.* **106**, 415–444 (1995).
- Prakriya, M. & Lewis, R. S. Potentiation and inhibition of Ca^{2+} release-activated Ca^{2+} channels by 2-aminoethylidiphenyl borate (2-APB) occurs independently of IP_3 receptors. *J. Physiol. (Lond.)* **536**, 3–19 (2001).
- Chung, S. C., McDonald, T. V. & Gardner, P. Inhibition by SK&F 96365 of Ca^{2+} current, IL-2 production and activation in T lymphocytes. *Br. J. Pharmacol.* **113**, 861–868 (1994).
- Eray, M., Matto, M., Kaartinen, M., Andersson, L. & Pelkonen, J. Flow cytometric analysis of apoptotic subpopulations with a combination of annexin V-FITC, propidium iodide, and SYTO 17. *Cytometry* **43**, 134–142 (2001).
- Graber, M. N., Alfonso, A. & Gill, D. L. Ca^{2+} pools and cell growth: arachidonic acid induces recovery of cells growth-arrested by Ca^{2+} pool depletion. *J. Biol. Chem.* **271**, 883–888 (1996).
- Ferrari, D. *et al.* Endoplasmic reticulum, Bcl-2 and Ca^{2+} handling in apoptosis. *Cell Calcium* **32**, 413–420 (2002).
- Manji, S. S. *et al.* STIM1: a novel phosphoprotein located at the cell surface. *Biochim. Biophys. Acta* **1481**, 147–155 (2000).
- Dolmetsch, R. E. & Lewis, R. S. Signaling between intracellular Ca^{2+} stores and depletion-activated Ca^{2+} channels generates $[\text{Ca}^{2+}]_i$ oscillations in T lymphocytes. *J. Gen. Physiol.* **103**, 365–388 (1994).
- Liou, J. *et al.* STIM is a Ca^{2+} sensor essential for Ca^{2+} -store-depletion-triggered Ca^{2+} influx. *Curr. Biol.* **15**, 1235–1241 (2005).
- Fanger, C. M. *et al.* Calcium-activated potassium channels sustain calcium signalling in T lymphocytes, selective blockers and manipulated channel expression levels. *J. Biol. Chem.* **276**, 12249–12256 (2001).

Supplementary Information is linked to the online version of the paper at www.nature.com/nature.

Acknowledgements We thank L. Forrest for assistance with cell culture; A. Yeromin, O. Safrina and S. Wei for help with $[\text{Ca}^{2+}]_i$ imaging; G. Chandy for the use of molecular reagents and laboratory facilities; C. Hughes for providing access to the Amaxa Nucleofector; A. Kolski-Andreaco for the gift of pAc5.1/EGFP; K. Knowlton and D. Summers-Torres from the Department of Medicine, University of California, San Diego for help with deconvolution immunofluorescence microscopy; and P. J. DiGregorio, G. Velicelebi, M. Lioudyno, J. Hall and Y. Li for discussion. Confocal microscopy was performed at the Optical Biology Shared Resource, supported by a Developmental Biology Center and Cancer Center Support Grant at the University of California, Irvine. This work was supported by grants from the National Institutes of Health (to M.D.C. and M.H.E.) and by a fellowship from the Pulmonary Hypertension Association (to Y.Y.).

Author Information Reprints and permissions information is available at ngp.nature.com/reprintsandpermissions. The authors declare no competing financial interests. Correspondence and requests for materials should be addressed to M.D.C. (mcahalan@uci.edu).